

Projections of the Pontine Nuclei to the Cochlear Nucleus in Rats

MATTHIAS OHLROGGE,¹ JOHN R. DOUCET,¹ AND DAVID K. RYUGO^{1,2*}

¹Departments of Otolaryngology-Head and Neck Surgery, Center for Hearing Sciences, Johns Hopkins University School of Medicine, Baltimore, Maryland 21205

²Department of Neuroscience, Center for Hearing Sciences, Johns Hopkins University School of Medicine, Baltimore, Maryland 21205

ABSTRACT

In the cochlear nucleus, there is a magnocellular core of neurons whose axons form the ascending auditory pathways. Surrounding this core is a thin shell of microneurons called the *granule cell domain* (GCD). The GCD receives auditory and nonauditory inputs and projects in turn to the dorsal cochlear nucleus, thus appearing to serve as a central locus for integrating polysensory information and descending feedback. Nevertheless, the source of many of these inputs and the nature of the synaptic connections are relatively unknown. We used the retrograde tracer Fast Blue to demonstrate that a major projection arises from the contralateral pontine nuclei (PN) to the GCD. The projecting cells are more densely located in the ventral and rostral parts of the PN. They also are clustered into a lateral and a medial group. Injections of anterograde tracers into the PN labeled mossy fibers in the contralateral GCD. The terminals are confined to those parts of the GCD immediately surrounding the ventral cochlear nucleus. There is no PN projection to the dorsal cochlear nucleus. These endings have the form of bouton and mossy fiber endings as revealed by light and electron microscopy. The PN represent a key station between the cerebral and cerebellar cortices, so the pontocochlear nucleus projection emerges as a significant source of highly processed information that is introduced into the early stages of the auditory pathway. The cerebro-pontocerebellar pathway may impart coordination and timing cues to the motor system. In an analogous way, perhaps the cerebro-pontocochlear nucleus projection endows the auditory system with a timing mechanism for extracting temporal information. *J. Comp. Neurol.* 436: 290–303, 2001. © 2001 Wiley-Liss, Inc.

Indexing terms: audition; granule cells; mossy fibers; synapse

The auditory system has been described with an organizing principle in which a core part conducts the ascending auditory information to cortex and faithfully represents the acoustic stimulus (Graybiel, 1974; Casseday et al., 1976; Ryugo, 1976). This core is surrounded by a shell that receives descending input from higher auditory centers as well as input from nonauditory parts of the brain. Feedback control from higher auditory centers is transferred through the shell region to the core (Mitani et al., 1983; Winer et al., 1998). Nonauditory information that is used to facilitate certain aspects of hearing is integrated by way of the shell (Ryugo, 1976; Huffman and Henson, 1990). Although the nature of this core-shell concept had usually been reserved for levels of the system above the midbrain, recent work has revealed that multimodal and descending inputs to the auditory system begin as early as the cochlear nucleus (CN; Itoh et al., 1987; Weinberg and Rustioni, 1987; Wright and Ryugo, 1996). The CN exhibits

this basic core-shell structure, in which the anterior and posterior ventral cochlear nucleus (VCN) and the dorsal cochlear nucleus (DCN) represent the core. The shell comprises the granule cell domain (GCD) overlying the VCN and separating VCN and DCN. To gain a better understanding of this shell in CN function, a first step is to identify the source of inputs to the GCD.

The synaptic endings of type I auditory nerve fibers terminate as part of the ascending auditory pathway in

Contract grant sponsor: NIH/NIDCD; Contract grant number: DC04395; Contract grant number: DC00232; Contract grant number: DC04505.

*Correspondence to: David K. Ryugo, Center for Hearing Sciences, JHU School of Medicine, 720 Rutland Avenue, Baltimore, MD 21205. E-mail: dryugo@bme.jhu.edu

Received 28 September 2000; Revised 26 March 2001; Accepted 11 May 2001

the core of the cochlear nucleus. These rapidly conducting, myelinated axons convey acoustic information to the brain via the auditory nerve. In contrast, the shell represented by the GCD receives input from type II auditory nerve fibers (Brown et al., 1988a; Hurd et al., 1999). These unmyelinated auditory nerve fibers most likely carry modulating signals or information about the status of the organ of Corti, because they originate from outer hair cells. The GCD also receives inputs from multiple higher auditory centers, such as the superior olivary complex (Brown et al., 1988b), the inferior colliculus (Caicedo and Herbert, 1993), and the auditory cortex (Feliciano et al., 1995; Weedman and Ryugo, 1996). Ascending terminals in the GCD arise from neurons of the spinal trigeminal nucleus (Itoh et al., 1987), the cuneate nucleus (Weinberg and Rustioni, 1987; Wright and Ryugo, 1996), and the vestibular nuclei (Burian and Goesttner, 1988). Granule cells influence the output of the DCN by way of parallel fibers contacting the apical dendrites of pyramidal cells (Mugnaini et al., 1980a; Manis, 1989; Saadé et al., 1989; Young et al., 1995). Granule cell influence on VCN output has not been shown. In addition to the known inputs to the GCD, ultrastructural studies have revealed multiple terminals within the GCD whose origins have not been determined (Mugnaini et al., 1980b). Of these, there are many so-called mossy fibers, some of which originate in the cuneate nucleus (Wright and Ryugo, 1996). Mossy fibers have a characteristic appearance, being relatively large (10–15 μm in diameter), making asymmetric synaptic contacts with several postsynaptic dendrites (Weedman and Ryugo, 1996; Weedman et al., 1996), and containing round synaptic vesicles. They have been so named because their morphology is similar to that of mossy fiber terminals in the cerebellar cortex.

The purpose of the present study was to determine the origin of some of these mossy fibers. This task represents a step towards a better understanding of multimodal integration at the level of the cochlear nucleus. Retrograde and anterograde tracing techniques were used to reveal a novel projection to the GCD and to demonstrate that a number of mossy fibers originate in the contralateral pontine nuclei (PN). Previously published observations on PN anatomy and physiology will be considered to develop ideas of possible functions of this pontocochlear nucleus projection. Some of these results were presented in abstract form at the 23rd annual Midwinter Research Meeting of the Association for Research in Otolaryngology, February 20–24, 2000.

MATERIAL AND METHODS

Animals and animal preparation

Male Sprague Dawley rats (250–300 g) from Charles River were used for all experiments. Animals were deeply anesthetized by intraperitoneal injection of sodium pentobarbital (45 mg/kg body weight), and oral secretions were blocked by 0.05 mg intramuscular injections of atropine sulfate. Surgery was performed only after animals were areflexic to tail or paw pinches. All procedures were in accordance with the guidelines and had the approval of the Animal Care and Use Committee of the Johns Hopkins School of Medicine.

Retrograde experiments

An incision by scalpel was made to the skin on the posterior surface of the skull and the soft tissue scraped away. An opening in the skull was made using drill and rongeurs, and the dura covering the cerebellum was cut. That part of the cerebellum overlying the left CN was aspirated to expose the characteristic smooth and shiny surface of the DCN. Fast blue (Sigma, St. Louis, MO) was injected into the lateral region of the granule cell lamina separating the VCN and DCN by direct visual control using an operating microscope. An injection of an aqueous solution containing 3% Fast Blue (20–60 nl) was made through a glass micropipette (30 μm inner diameter; ID) using an oocyte digital microdispenser (Nanoject Variable; Drummond Scientific Co., Broomall, PA). Injections were delivered at a rate of 1–5 nl/minute over a time period of 20 minutes. At the end of the injection, the pipette was left in place for an additional 5 minutes before withdrawal. The hole in the skull was filled with gelfoam, the incision was sutured, and the animals were allowed to recover. Four to six days later, animals were administered a lethal IP dose of sodium pentobarbital (100 mg/kg) and then transcardially perfused with ~ 50 ml of 0.1 M phosphate-buffered saline, pH 7.4, followed by 300 ml of 10% formalin in the same buffer. After perfusion the brain was removed from the skull and allowed to postfix for 1 hour at 4°C. The brain was then transferred into a 20% sucrose solution in phosphate buffer, pH 7.4, overnight at 4°C. The brainstem was sectioned on the next day on a freezing microtome at a thickness of 50 μm . Every other section was mounted in serial order on clean glass slides and air dried, then coverslipped in Krystalon mounting medium (Harleco; EM Science, Gibbstown, NJ). Labeled cells were located and photographed on the same day using a fluorescent microscope at a wavelength of 360 nm and a cooled, three-chip RGB digital CCD camera (C5810; Hamamatsu) at $\times 100$, $\times 200$, or $\times 400$ magnification.

Anterograde experiments

Anesthetized animals were positioned into a stereotaxic frame, the skin and soft tissue over the parietal bone were reflected, and a 2-mm-diameter hole was drilled in the skull. A glass pipette (30 μm ID), filled with a mixture of 2.5% biotinylated *Phaseolus vulgaris* leucoagglutinin (PHA-L; Vector Laboratories, Burlingame, CA) and 2.5% PHA-L (Vector Laboratories) in phosphate buffer, pH 7.9, was lowered into the brain using a micromanipulator. The pipette was positioned according to stereotaxic coordinates so that its tip was placed in the left PN. An injection of 200 nl was made at a rate of 10 nl/minute using the Drummond microdispenser. Pipettes were left in place for 5 minutes after injection. The skin was sutured, and the animals were given time to recover. After 7–10 days, the animals were again deeply anesthetized with a lethal dose of pentobarbital (100 mg/kg body weight) and then transcardially perfused with 20 ml of 0.1 M phosphate-buffered saline, pH 7.4, followed by 4% paraformaldehyde in phosphate buffer, pH 7.4. The brain was removed from the skull and postfixed for 1 hour at 4°C. Then, the tissue was embedded in gelatin-albumin mixture for stability while sectioning and cut into coronal sections (50 μm thickness for the CN or 75 μm for the pons) on a Vibratome. Sections containing the CN or PN were pro-

cessed differently to optimize visualization of the injection site and the labeled fibers.

In our experiments, we observed that, after injections of biotinylated PHA-L into the pontine nuclei, we could not stain the injection site. It was possible, however, to locate the tissue damage by the pipette tip, so we could identify the location of the injection site but could not determine its size. We solved this problem by adding PHA-L to the tracer solution and visualizing the injection site using antibodies and an immunohistochemical reaction with 3,3-diaminobenzidine (DAB). Because we applied the tracer mixture by pressure, we infer that the injection site recovered by the visualization of the DAB reaction product to PHA-L also represented the biotinylated PHA-L injection site. We have no explanation for why the biotinylated PHA-L injection site was not detectable in the PN, in that the same protocol revealed intense biotinylated PHA-L staining of axons and terminals in the CN. Reports on the properties of PHA-L and biotinylated PHA-L suggest that the same tracer can behave differently when applied in different areas of the brain (Schofield, 1990). Our observation might be due to this phenomenon.

CN sections were incubated overnight in avidin-biotin-peroxidase complex (ABC Elite; Vector Laboratories) in 0.1 M phosphate-buffered saline, pH 7.4, at 4°C. On the next day the sections were rinsed twice in phosphate buffer, pH 7.4, and twice in 0.05 M cacodylate buffer, pH 7.2. The label was developed with 0.0125% DAB, 0.25% nickel ammonium sulfate, and 0.35% imidazole in 0.05 M cacodylate, pH 7.2. Sections were preincubated in DAB solution for 10 minutes without hydrogen peroxide and then incubated in fresh DAB with 0.02% hydrogen peroxide for an additional 15 minutes. Sections were mounted on gelatin-coated microscope slides, counterstained with cresyl violet, and coverslipped with Permount.

Sections containing the PN were processed using the following procedures. Unless otherwise stated, all immunocytochemical processing was performed at room temperature in Tris-buffered saline (TBS; 0.05 M, pH 7.6). Sections were washed in TBS, pH 7.6, blocked in 5% nonfat dry milk for 2 hours, and incubated overnight in rabbit anti-PHA-L (Vector Laboratories) at a concentration of 1:2,000. Membranes were permeabilized by the addition of 0.1% Photo-Flo (Kodak) to both the primary and the secondary antibody solutions. On the next day, sections were washed three times in TBS and incubated in goat anti-rabbit immunoglobulin (IgG) secondary antibody (1:50) in TBS for 2 hours. After three more washes in 0.05 M TBS, pH 7.6, sections were treated with rabbit peroxidase antiperoxidase at 1:400 for 1 hour. Washes in TBS were followed by a 5–10 minute incubation in 0.05% DAB and 0.015% H₂O₂ in Tris buffer (0.05 M; pH 7.6). Sections were washed further, mounted on gelatin-coated slides, air dried, counterstained in cresyl violet, and coverslipped.

Because the DAB reaction product is electron dense, we could dissect specific regions containing labeled mossy fiber endings from the main tissue sections and reembed the smaller pieces for ultrathin sectioning and analysis with an electron microscope. Light microscopic maps of these smaller blocks were made for orientation purposes, using blood vessels and labeled structures as landmarks. Serial ultrathin sections were collected on Formvar-coated slotted grids and photographed with a Jeol 100CX electron microscope.

Data analysis

For the retrograde studies, only rats with injection sites restricted to the CN were included ($n = 6$). Verification of the injection site consisted of microscopic analysis of serial sections spanning the entire rostral caudal extent of the CN. Every other section was drawn through the CN using a microscope and drawing tube (total magnification $\times 63.5$). The perimeter of the GCD was outlined and its surface area calculated (The Image Processing Tool Kit; Reindeer Games, Inc., Gainesville, FL). The area for each section was multiplied by section thickness (0.05 mm) to obtain GCD volume, the resulting value doubled to compensate for the missing intervening section and summed to estimate total GCD volume. Outlines were digitized and scaled to match the corresponding photomicrograph, and the injection site visible in each section was copied to its corresponding drawing. The area of overlap between injection site and GCD was calculated, and the total injection site volume in the GCD was determined.

We also examined nearby adjacent structures, such as the inferior cerebellar peduncle, trigeminal nerve root, vestibular nerve root and nuclei, and descending tract and nucleus of the trigeminal nerve. Included in this analysis were various nuclei known to give rise to axons traveling in the nearby tracts, such as the inferior olive projecting through the inferior cerebellar peduncle and Scarpa's ganglion projecting through the vestibular nerve. In this way we could be confident that there was not a "fibers of passage" contamination problem.

The distribution of retrogradely labeled cell bodies in the PN was determined using photomontages of the PN. Each montage was constructed from multiple digitized images using standard software (Adobe Photoshop 5.0). The perimeters and regional boundaries of individual sections were digitized and superimposed on the montages, and labeled cells were plotted directly on the drawing and counted. Every labeled cell in the PN was counted and noted for its position ipsilateral or contralateral to the injection site. We used cell counts to determine the relative projection with respect to side. We did not calculate total cell counts, because that value would necessarily be determined by the size of the injection site.

Analysis of anterogradely labeled fibers and terminals was conducted using light and electron microscopy. Only animals with injection sites verified to be within the PN ($n = 5$) were used. Alternate sections were drawn through the entire PN using a microscope and drawing tube (total magnification $\times 63.5$). The PN borders were established by cytoarchitectonic criteria (Mihailoff et al., 1981) and scaled to matching micrographs containing the injection sites, and injection sites were copied to the drawings. PN and injection volumes were calculated as described above.

DAB reaction product filled fibers and terminals in a continuous manner. Labeled fibers were followed by light microscopy through serial sections, away from the PN and into the CN, where they terminated as large swellings in the granule cell domain. Selected sections were outlined and terminals were plotted on the drawn sections using tissue landmarks and a drawing tube. Labeled structures were photographed using a CCD camera at various levels of magnification.

RESULTS

Retrograde experiments

GCD injections. The presence of mossy fiber endings in the GCD has been known for some time, but their origin has not. Fast Blue was injected into the granule cell lamina, the part of the GCD that separates the VCN and

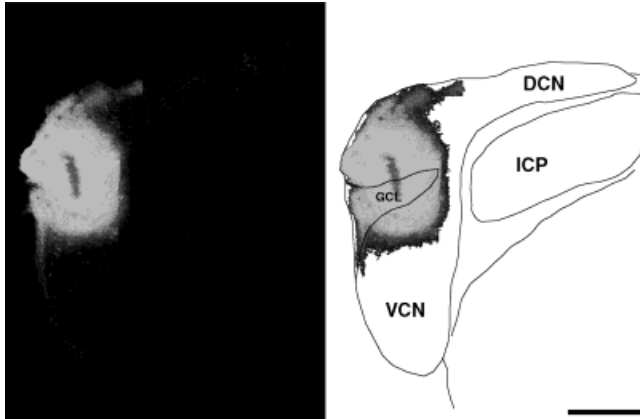


Fig. 1. Representative injection site of Fast Blue into the cochlear nucleus. **Left:** Fluorescent photomontage through the injection site illustrating the distribution of Fast Blue. **Right:** Drawing of the nucleus in the coronal plane with the injection site included. The injection is centered in the granule cell lamina separating the VCN and DCN. The distribution of the tracer is confined to the anatomical boundaries of the cochlear nucleus. GCL, granule cell lamina; ICP, inferior cerebellar peduncle; VCN, ventral cochlear nucleus; DCN, dorsal cochlear nucleus. Scale bar = 0.5 mm.

DCN, to determine the cell bodies of origin that give rise to projecting terminals (Fig. 1). This part of the GCD is the thickest here and represents the largest continuous extent of granule cells in the CN. The GCD volume was calculated for 10 CN from these rats. The volumes ranged from 0.175 to 0.271 mm³, with a mean (\pm SD) of 0.227 ± 0.03 mm³. In six rats, injections were centered precisely within the lamina and did not extend outside the boundaries of the CN (Fig. 1). The injection site volumes within the GCD ranged from 0.092 to 0.056 mm³, with a mean of 0.069 ± 0.02 mm³. This value reveals that the injection site filled on average approximately 28% of the GCD volume. The inferior cerebellar peduncle (ICP) lies under the DCN and medial to the VCN and carries fibers traveling into the cerebellum that originate in the brainstem and spinal cord. Fibers in the ICP, however, do not originate in the PN. Thus even leakage into the ICP should not influence the label in the PN.

Labeled neurons of the PN. GCD injections produced labeled cells bilaterally in the PN (Fig. 2). The predominance of labeling was on the contralateral side, where numerous cell bodies of various sizes and shapes contained retrograde label. From alternate sections, we counted from 362 to 1,368 ipsilaterally labeled cells and from 1,192 to 3,987 contralaterally labeled cells. Approximately 80% of all labeled PN cells were distributed on the side contralateral to the injection site. This ratio was remarkably consistent, ranging from 0.74 to 0.86, with a mean of 0.804 ± 0.047 . There was a striking difference in intensity of label between individual cells on the contralateral side. Some cells were labeled very brightly, whereas others were clearly but lightly labeled (Fig. 3). In spite of these intensity differences, all labeled cells were analyzed similarly. The labeled cells within the contralat-

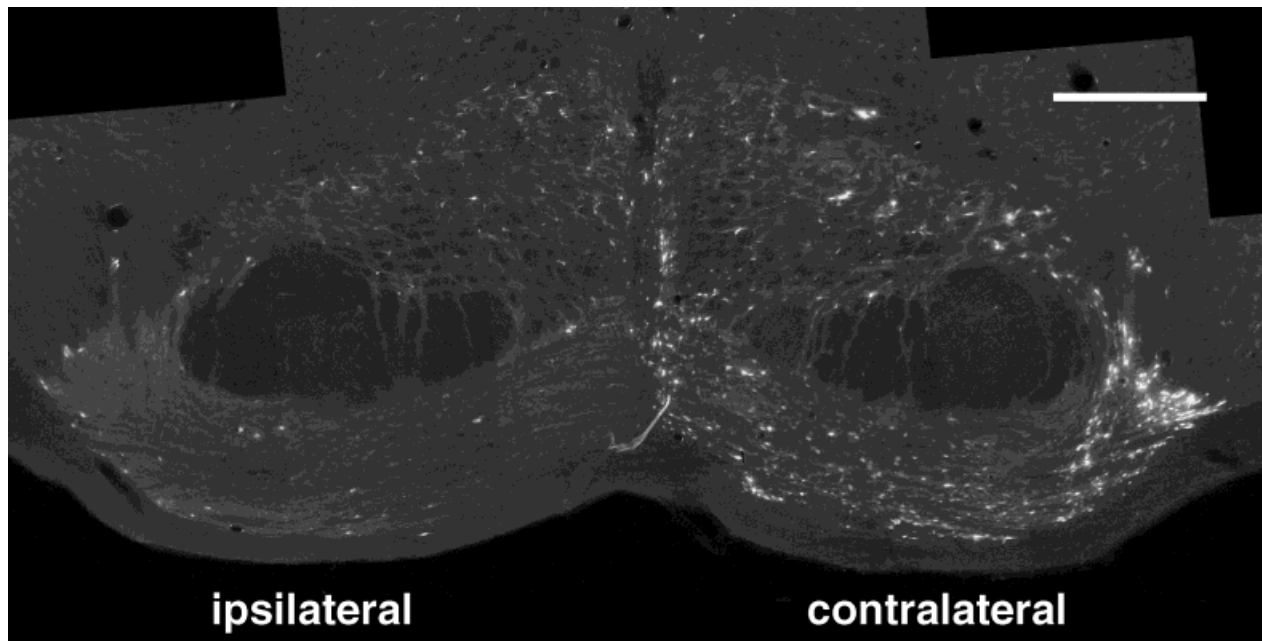


Fig. 2. Representative fluorescent photomontage of a coronal section through the pontine nuclei (experiment 5/5/00 A). Fast Blue was injected into the left granule cell domain (GCD). Labeling is mostly contralateral to the injection site, and projecting cells tend to be concentrated in a lateral and medial cluster. Scale bar = 0.5 mm.

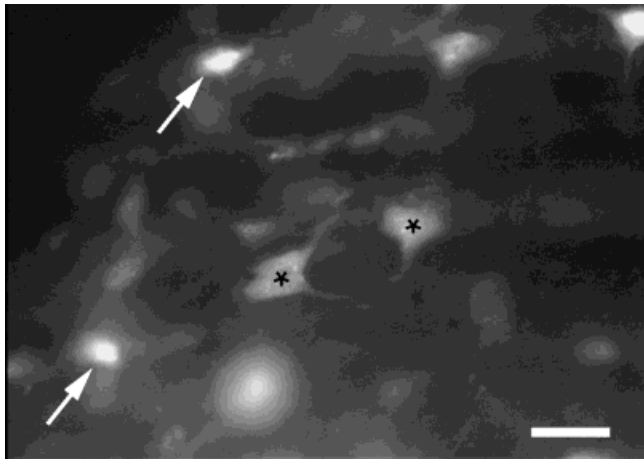


Fig. 3. Fluorescent photomicrograph of retrogradely labeled cells in the pontine nuclei (PN) following a cochlear nucleus injection. Some cells showed intense label (arrows), whereas others, although clearly labeled, showed less intense label (asterisks). Labeled cells exhibited variations in somatic size and shape, an observation consistent with what has been previously reported for the PN (Mihailoff et al., 1981). Scale bar = 20 μm .

eral PN were not evenly distributed but exhibited distinct clustering in some areas. Labeled cells were distributed more densely in the ventral parts of the PN than in the dorsal parts. In the rostral PN, cells seemed to be evenly distributed throughout the PN; more caudally, labeled cells segregated into aggregations that could be followed through consecutive sections, forming elongated patches or columns (Fig. 4). These columns were not consistently found in any particular part of the PN except for a medial cluster.

The stained cells of the ipsilateral PN were less intensely, but more uniformly, stained. They did not exhibit any distinct clustering. In addition to the cells in the PN, there are labeled cells in other parts of the brain. For example, we observed labeled cells in the contralateral inferior colliculus and the superior olive bilaterally. Those projections, however, have been described previously (see, e.g., Shore et al., 1991; Shore and Moore, 1998; Schofield and Cant, 1999) and will not be discussed further here except to say that they served as positive controls for our methods.

There has been discussion that, in the dorsal pontine region, it is not always possible to distinguish between groups of cells that are part of the PN and groups that represent the nucleus reticularis tegmenti pontis (NRTP; Mihailoff et al., 1981). PN neurons tend to have ovoid somata, whereas NRTP neurons tend to be larger, with intensely basophilic somata. The dorsally located stained cells in our experiments tended to be small, and we did not stain them with basophilic dyes. Because they were also relatively infrequent, for economy's sake we grouped them with the PN.

Anterograde experiments

The pontine nuclei. Results for the anterograde experiments were collected from 10 animals. Five animals had injections confined to the PN that contained a mixture of PHA-L and biotinylated PHA-L and provide the projec-

tion data. The PN represent an accumulation of neurons making up the gray matter of the basal pons. Subdivisions of this cell group have been described but for mostly descriptive rather than functional purposes (Mihailoff et al., 1981). These divisions include neuron clusters located medially, ventrally, and laterally to the cerebral peduncle and neurons lying adjacent to the peduncle defined as part of the peduncular nucleus. Neurons with cell bodies of various sizes are distributed throughout the region without any particular order. The mean volume of the PN on one side was calculated as $1.81 \pm 0.2 \text{ mm}^3$, with a range of $1.58\text{--}2.01 \text{ mm}^3$ ($n = 10$). Resembling the cat, rabbit (Brodal and Jansen, 1946), and opossum (King et al., 1968), the rat does not exhibit any specific cytoarchitectonic features that characterize the major pontine subdivisions (Mihailoff et al., 1981).

Running longitudinally through the pontine nuclei are two main fiber tracts, the longitudinal fasciculus of the pons (LFP; a continuation of cortical axons that make up the cerebral peduncles) and the medial lemniscus. The LFP carries efferent information to motor neurons in the medulla and spinal cord as part of the corticobulbar and corticospinal tracts, respectively. No afferent fiber system has been described for the LFP so far. The medial lemniscus carries second-order sensory axons that arise from the dorsal column nuclei.

Pontine projections. In two cases (11/3/99 D and 11/3/99 B), the injection site was completely confined to the pontine nuclei (Figs. 5, 6). The limits of the PN were drawn using the boundaries of areas with high cell density, and the outlines were consistent with those of a rat stereotaxic atlas (Paxinos and Watson, 1982). In two other cases (9/29/99 C and 11/3/99 A), the injection site included part of the LFP. We found, however, that the results of these experiments were essentially identical to those when the injection was anatomically limited to the PN. These showed labeled endings in the contralateral GCD of the CN, excluding the DCN, and no labeling was seen in the magnocellular core regions of the CN. In one case (4/27/99 C), the injection site was on the dorsal border of the PN but produced labeling with the same pattern as that from pure PN injections. The volume of the injection sites contained within the PN ranged from 0.033 to 0.096 mm^3 , with a mean of $0.063 \pm 0.03 \text{ mm}^3$. The variation in amount and location of tracer injected in these experiments did not qualitatively change the nature or pattern of label in the CN. Thus we inferred that the injections included in our database were limited to regions of the PN projecting to the GCD.

In the five cases with injections in the PN, labeled fibers were followed to the GCD, where they branched and distributed terminals (Fig. 7). No label was found in the DCN or in the magnocellular core of the VCN. The fibers appeared to reach the CN by way of the intermediate acoustic stria, where they proceeded to disperse into their separate ways. That is, they did not distribute themselves as a discrete group within the anatomical boundaries of the CN. Rather, they ran as individuals through the granule cell lamina between VCN and DCN and continued into the layer of granule cells that surround the dorsolateral surface of the VCN. There, they ran parallel to the VCN surface. The labeled fibers were relatively thin, typically between 0.5 and $1.0 \mu\text{m}$ in thickness. During their passage, the fibers branched and gave rise to en passant and terminal swellings (Fig. 8).

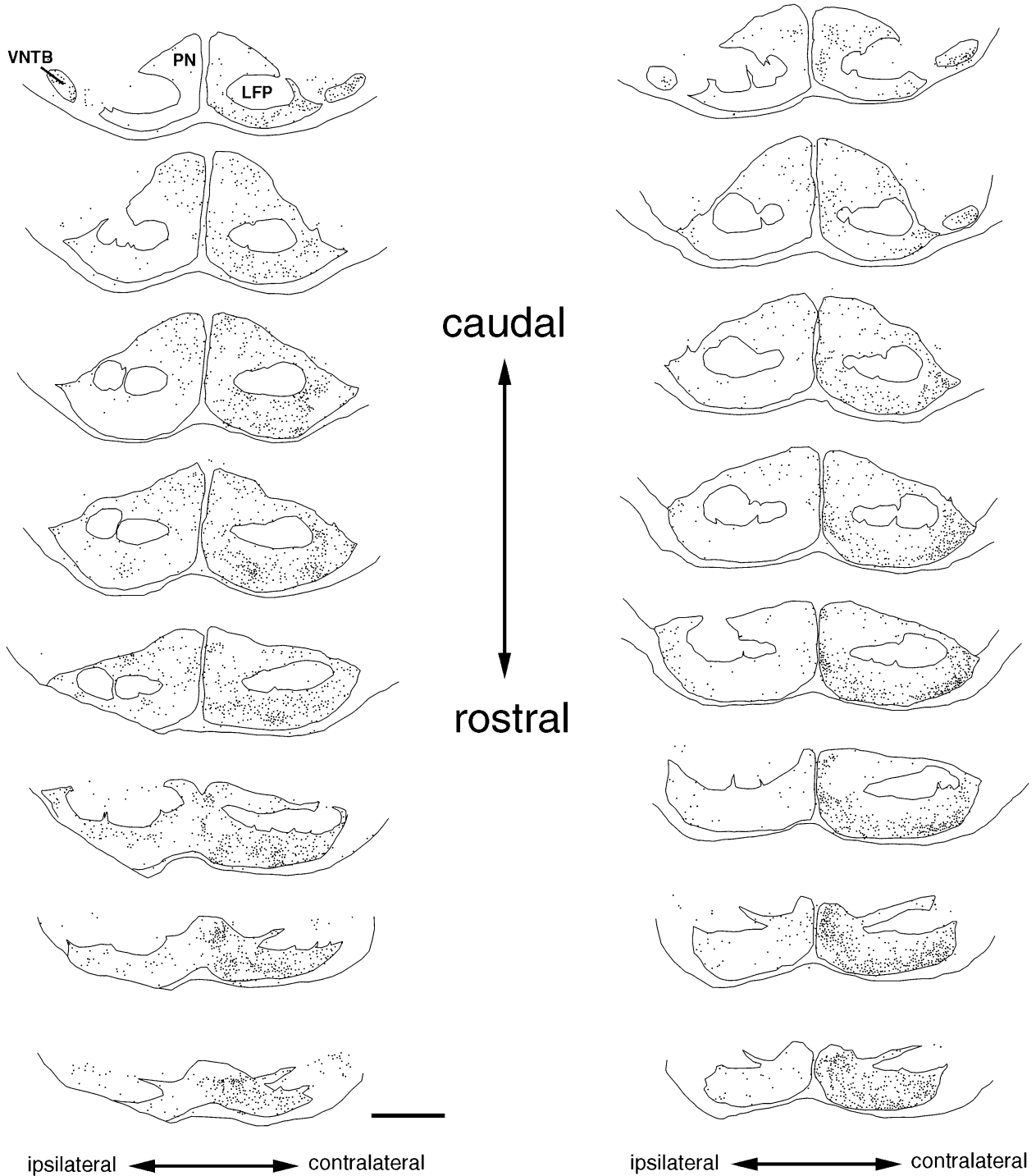


Fig. 4. Drawings of evenly spaced, representative coronal sections through the pontine nuclei (PN) of two different animals (11/17/99A on left, 5/5/00A on right). Every labeled cell is represented by a dot in the drawing. Different intensity of label has not been considered. As in all cases, the contralateral PN shows a significantly greater num-

ber of labeled cells than the ipsilateral side. In addition, more cells are labeled in the rostral and ventral regions of the PN. In the caudal PN, both cases show a lateral and a medial area with a greater density of labeled cells. LFP, longitudinal fasciculus of the pons; VNTB, ventral nucleus of the trapezoid body. Scale bar = 1 mm.

These swellings were rather variable in size and shape (Fig. 9). This variation in ending characteristics does not seem to correlate with their location within the GCD. The

small endings ranged from 1 to 3 μm in diameter, tended to be smooth and round, and resembled typical bouton endings found throughout the central nervous system. At

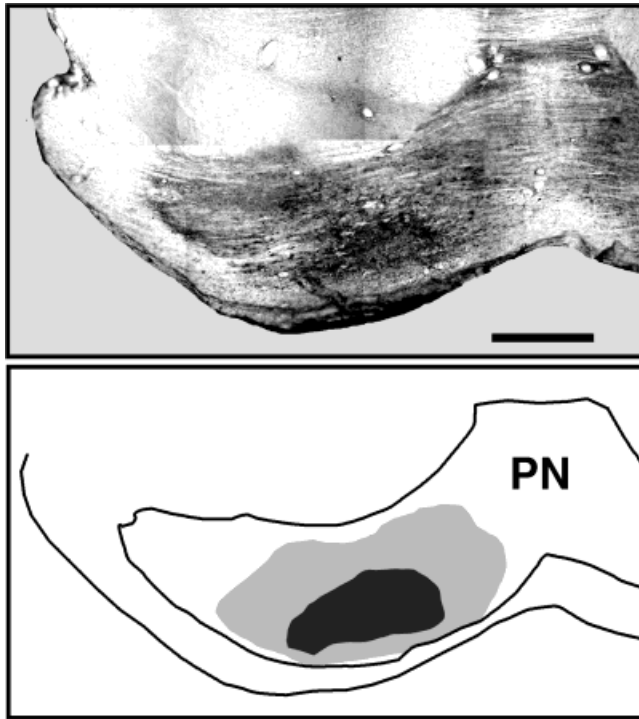


Fig. 5. Photomontage of an injection site (case 11/3/99D) of a PHA-L and biotinylated PHA-L cocktail in the pontine nuclei (PN; **top**). The PHA-L has been processed with DAB, revealing that the injection site is confined within the boundaries of the PN. A drawing illustrating the injection site is shown on the **bottom**, where solid indicates the center of the injection site and shaded indicates the halo. Scale bar = 0.5 mm.

the other extreme, endings were relatively large (5–15 μm in diameter) and irregular in shape. These latter endings closely resembled the appearance of so-called mossy fibers of the cerebellum (see, e.g., Ramón y Cajal, 1909) and mossy fibers of the GCD that arise from the cuneate nucleus (Wright and Ryugo, 1996). In addition to being large, they had irregular edges and bleb-like protrusions, arose as either en passant or terminal swellings, and were distributed in regions with high density of granule cells. They did not appear to make contact with resident cell bodies.

Ultrastructural characteristics. We examined a number of large labeled endings from the GCD with the electron microscope. Some of these endings were boutons (Fig. 10A), and others were mossy fibers (Fig. 10B). Boutons mostly contacted thin (<1.0 μm in diameter) dendritic profiles. Mossy fibers formed an eccentric structure incompletely surrounded by dendritic and axonal processes. Consistent with the light microscopic appearance, the labeled mossy fiber endings exhibited considerable variations in shape. The surrounding processes also varied. The labeled endings themselves exhibited the classic appearance of mossy fiber terminals in the CN, filled with round synaptic vesicles, numerous mitochondria, and prominent asymmetric synapses (Mugnaini et al., 1980a; Weedman et al., 1996; Wright and Ryugo, 1996). The pre- and postsynaptic densities are especially exaggerated by the DAB reaction product, helping to highlight the synaptic cleft. The labeled endings arising from the PN were

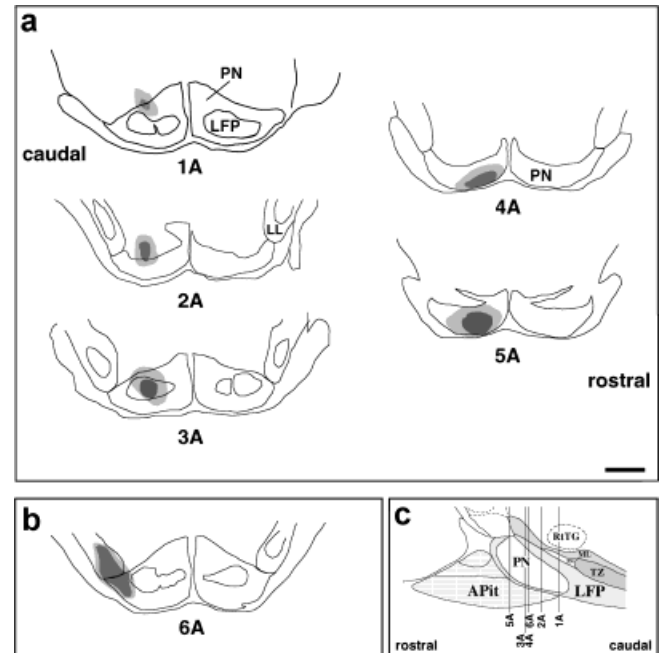


Fig. 6. Drawing tube reconstructions of PN injection sites used in this study. **a**: Sites that are limited to the pontine nuclei (PN) and that produced labeled terminals in the granule cell domain (GCD) of the cochlear nucleus. Each section is taken through the middle of the injection site. 1A, case 4/27/99C; 2A, case 9/29/99C; 3A, case 11/3/00AA; 4A, case 11/3/99D; 5A, case 11/3/99B. **b**: Example of an injection site (case 9/29/99a) that included part of the ventral nucleus of the trapezoid body (out of the plane of this section) and the lateral lemniscus. This case resulted in labeled terminals in the GCD and magnocellular parts of the cochlear nucleus. **c**: Parasagittal view of the pontine region showing the rostrocaudal location of injection sites. The vertical lines are placed through the center of each injection site and labeled with respect to part 6A. APit, anterior pituitary lobe; LFP, longitudinal fasciculus of the pons; LL, lateral lemniscus; ML, medial lemniscus; RtTG, reticulotegmental nucleus of the pons; TZ, trapezoid body. Scale bar = 1 mm.

typically filled with small, round synaptic vesicles, and the postsynaptic densities were either large and continuous (Fig. 10C) or segmented (Fig. 10B).

The dendrites contacted by labeled mossy fibers from the PN are not numerous, but there is a pattern to the synaptic relationships. The number of postsynaptic dendrites surrounding the mossy fiber is inversely related to its profile diameter. That is, a single postsynaptic dendrite tends to be large (1–2 μm in diameter). When there are two dendritic profiles, they are often close together and just a bit thinner (0.75–1.5 μm in diameter) than the single profile, as though they were branches near the main stalk. The thin dendritic profiles (0.3–0.8 μm in diameter) are typically separate from one another, resembling the distal portions of the granule cell dendritic claw. In addition, sometimes there are thin, finger-like dendritic processes that project into the mossy fiber, and these can be postsynaptic. We infer that the pontine mossy fibers form synaptic glomeruli with the distal dendrites of granule cells.

Injection sites outside the PN. In two cases that were rejected, the injection site included not only the PN but also the adjacent lateral lemniscus or the ventral nucleus

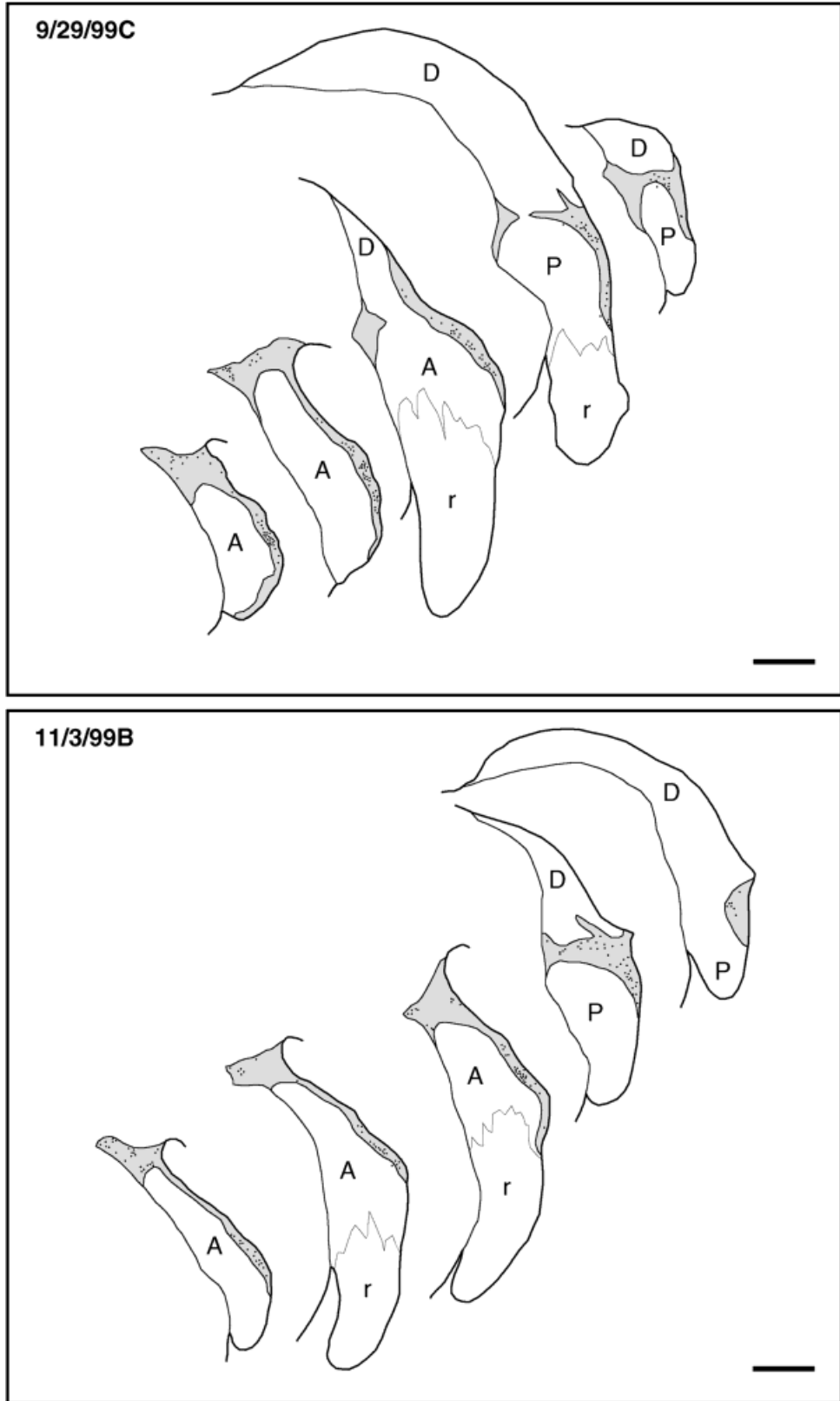


Fig. 7. Drawing tube reconstructions of equally spaced coronal sections through the cochlear nucleus (CN) of two representative animals. The granule cell domain (GCD) is shown in the shaded area. These drawings illustrate the distribution of labeled mossy fiber terminals originating from the contralateral pontine nuclei. Individual mossy fiber terminals are marked with a dot, and bouton endings are

not shown. Note that mossy fibers are confined to that part of the GCD overlying the ventral CN (VCN). No labeled endings were observed in the dorsal CN, but a few labeled terminals were located in the VCN, immediately beneath the GCD. A, anteroventral cochlear nucleus; D, dorsal cochlear nucleus; P, posteroventral cochlear nucleus; r, auditory nerve root. Scale bars = 0.5 mm.

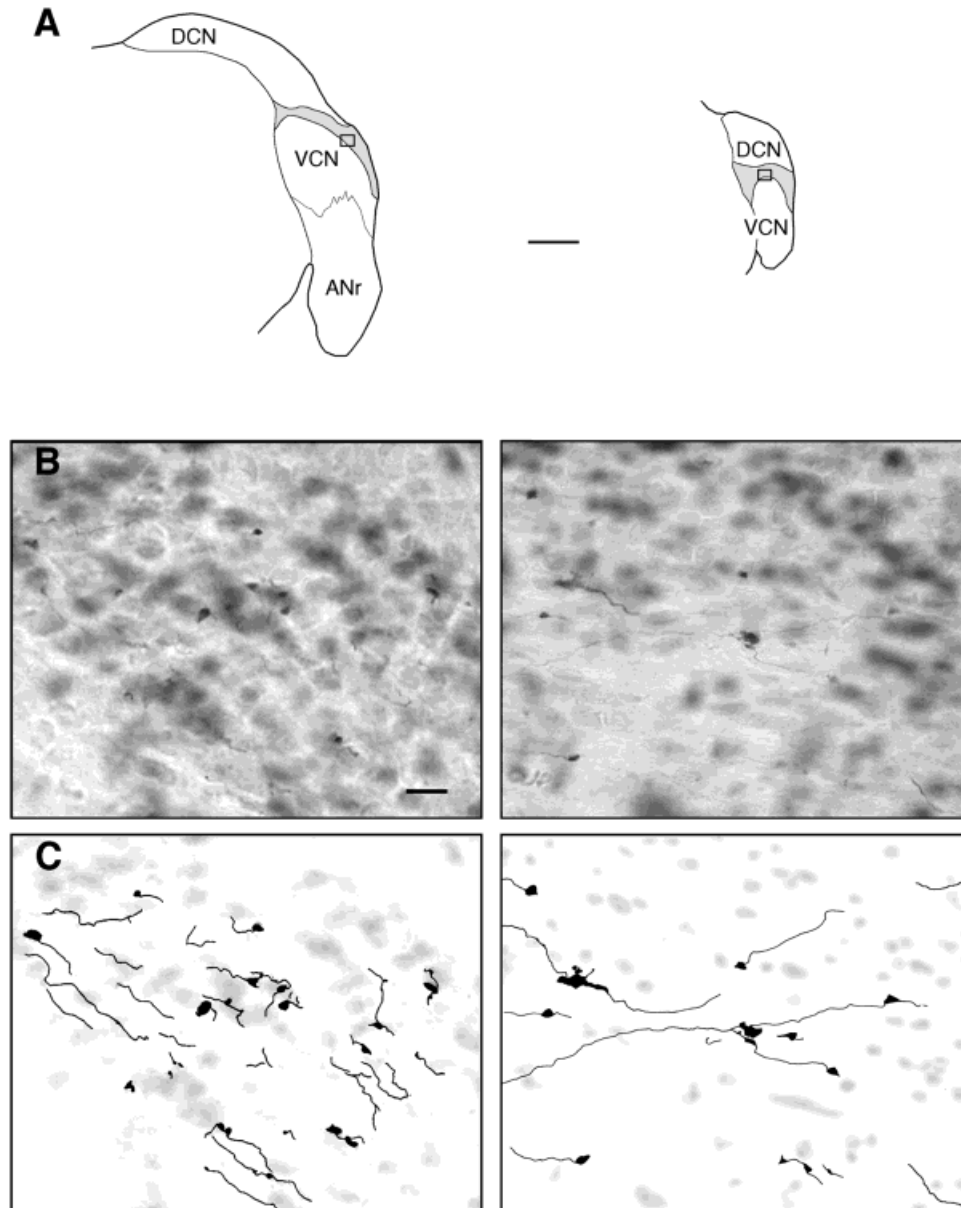


Fig. 8. Illustrations of mossy fiber endings in the granule cell domain (GCD). **A:** Drawing tube reconstructions of sections containing the GCD with box drawn around labeled mossy fiber terminals shown directly below. ANr, auditory nerve root. **B:** Photomicrographs of labeled mossy fibers, boutons, and fibers. **C:** Drawing tube reconstructions of labeled terminals and fibers (solid) in the cochlear nucleus (CN), corresponding to the photomicrographs shown directly above. Fibers run more or less parallel to the surface of the ventral CN

(VCN), terminating in irregularly shaped endings that are between 2 and 10 μm in diameter. The endings intermix with cell bodies (shaded) but do not appear to make somatic contact. The light microscopic appearance of these endings resembles that of mossy fibers previously described for the cochlear nucleus (Wright and Ryugo, 1996) and cerebellar cortex (Palay and Chan-Palay, 1974). Scale bar in A = 0.5 mm; scale bar in B = 10 μm for B,C.

of the trapezoid body (see Fig. 6b). These two experiments produced typical mossy endings in the GCD of the contralateral side. In addition, however, many endings including boutons were seen in the granule cell layer of the DCN as well as bilaterally in the magnocellular core of VCN and DCN. Those bouton endings were distinctly smaller (2–5 μm) than the mossy fiber endings described above. They exhibited a regularly smooth shape and occurred as en passant and terminal endings. In the DCN

they were distributed more densely towards the molecular layer and seemed to end in the neuropil rather than in proximity to cell bodies. In contrast, boutons in the VCN seemed to make contact with neuronal somata. Electron microscopic examination of these bouton endings throughout the VCN (results not shown) revealed a different appearance of those endings compared to the mossy endings. They made direct synaptic contact with cell bodies in the CN and contained pleomorphic synaptic vesicles. Thus,

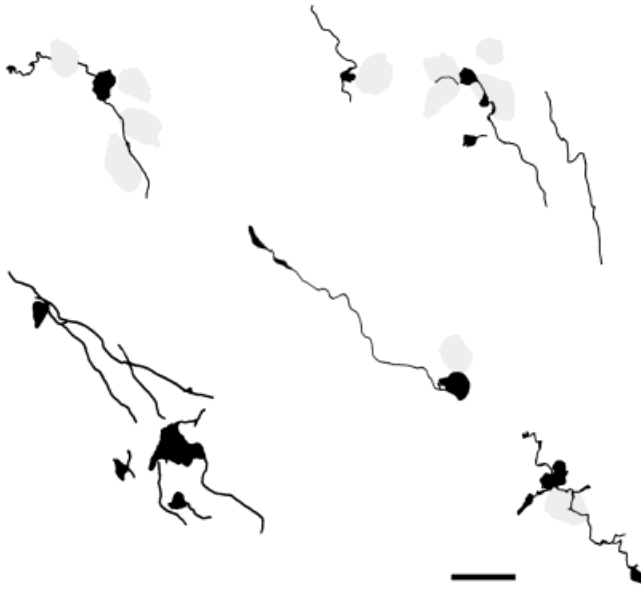


Fig. 9. High-magnification ($\times 100$ oil objective, NA 1.3) drawing tube reconstructions of typical mossy terminals in the granule cell domain. The diameters of these endings range from 4–12 μm (bouton endings have been omitted). Fibers run predominantly parallel to each other and to the surface of the ventral cochlear nucleus. Somata of granule cells are shown in the shaded areas. Scale bar = 10 μm .

when the injection site strayed into the nuclei of the lateral lemniscus or ventral nuclei of the trapezoid body, labeled endings exhibited distributions and ultrastructural features different from those arising from the purely PN injections.

Question of topographic projections. The PN injection sites were located in different rostral-caudal locations throughout the PN. Nevertheless, every injection produced labeled fibers and endings scattered throughout the GCD (see Fig. 7). The vast majority was located in the contralateral GCD, and only a few fibers and endings were observed ipsilaterally. Fibers and endings were restricted to the GCD or a surrounding region within 50 μm from the edge of the nucleus, also known to contain granule cells. On the basis of these data, we tentatively conclude that there is not a rostrocaudal topography in the projections to the GCD.

DISCUSSION

In this study we have shown that the PN give rise to a prominent projection to the granule cell domain of the CN. Although the projection is bilateral, the bulk of the projection goes to the contralateral CN. Thin fibers (1–1.5 μm in thickness) exit the PN, join the lateral lemniscus, and penetrate the CN through the intermediate acoustic stria. Upon entering the CN, individual fibers separate from the group, branch, and distribute en passant and terminal swellings to that part of the GCD associated with the VCN. The granule cell layer (layer 2) of the DCN receives no projection.

The origin of these PN projections exhibits an organized pattern, in that the involved neurons are not evenly distributed. The number of projecting cells decreases from

rostral to caudal and from ventral to dorsal. We also identified a lateral and a medial region in the contralateral PN that contains more projecting cells, especially with respect to the more central region between them.

The terminals themselves exhibit a wide range in size and shape. There are small swellings that are easily classified as boutons and large, irregularly shaped swellings that resemble the classic description of mossy fibers in the cerebellum. Electron microscopy revealed that both bouton and mossy fiber terminals contain round synaptic vesicles and form asymmetric membrane specializations with dendritic processes. The structural features of these synapses are similar to those reported for other mossy fibers of the CN (Mugnaini et al., 1980a; Weedman et al., 1996; Wright and Ryugo, 1996). The particular relationship of labeled mossy fibers to dendritic processes strongly suggests that the pontine neurons make excitatory connections with the dendritic claws of granule cells.

Specificity of PN projections

In two experiments, the injection sites extended from the dorsolateral corner of the PN into adjacent structures. In these cases, we observed labeling of fibers and bouton endings in the DCN and in the magnocellular part of the VCN. We also observed labeled axons and mossy fiber endings in the GCD, identical to the situation when injection sites were entirely contained within the PN. The most parsimonious interpretation of these results is that the GCD projection arose from the PN, and the new projection arose from the adjacent nuclei into which the injection site spread.

There are several auditory structures in the immediate vicinity of the PN. These include the ventral nucleus of the lateral lemniscus; the lateral, ventral, and medial nuclei of the trapezoid body; and the anterolateral periolivary nucleus or rostral periolivary region. Each of these regions receives input from the CN (Fernandez and Karapas, 1967; Glendenning et al., 1981; Warr, 1982; Kandler and Herbert, 1991), but the lateral and ventral nuclei of the trapezoid body are best known for their projections back to the CN (Elverland, 1977; Spangler et al., 1987; Warr and Beck, 1996). These projections to the CN do not include mossy fiber terminals in the GCD but do exhibit bouton terminals in the DCN and VCN (Sherriff and Henderson, 1994; Warr and Beck, 1996). Therefore, we infer that the labeled axons and terminals in the magnocellular core of the VCN and DCN in our experiments arise from the lateral and ventral nuclei of the trapezoid body, not from the PN.

Evidence for convergence of PN onto GCD

An issue in our data that merits further discussion is the clear asymmetry seen when comparing the relative "size" of the anterograde projections to that of the retrogradely labeled projecting neurons. Specifically, there is a seemingly sparse projection to the GCD from the PN, whereas there is a surprisingly large number of retrogradely labeled PN neurons following GCD injections. Our explanation lies in the relative difference in volume between the connected structures. The unilateral volume of the PN is nearly 10 times greater than the volume of the contralateral GCD, but the mean size of the injection sites at the two locations is statistically indistinguishable ($P = 0.85$), with that for PN equal to $0.063 \pm 0.03 \text{ mm}^3$, compared to $0.069 \pm 0.02 \text{ mm}^3$ for the GCD. Consequently, the

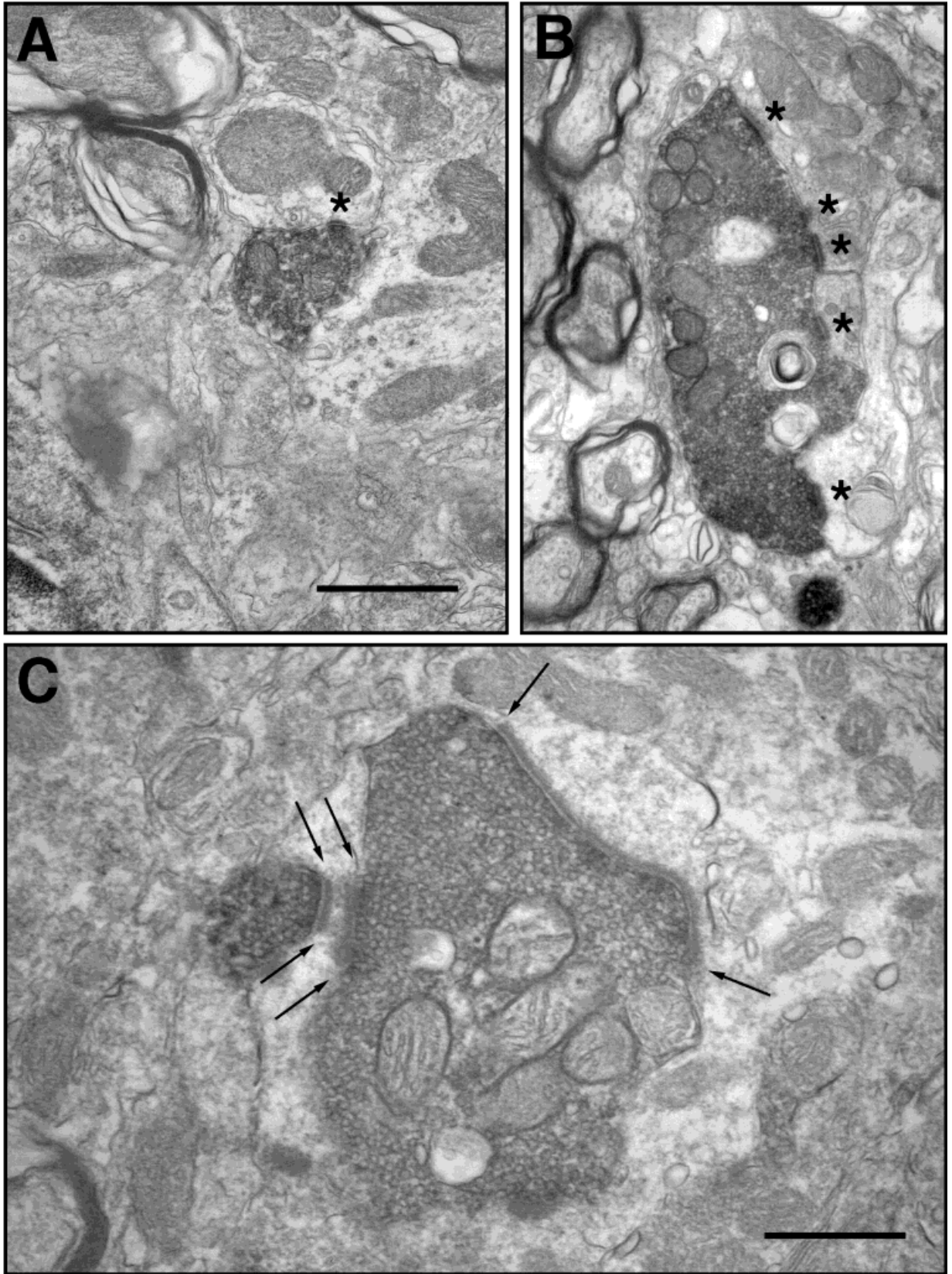


Figure 10

injection sites in the PN involved 3.5% of the structure (by volume), whereas that in the GCD involved 28.1% of the structure. Consequently, the injection sites in the PN involved only a small number of the total projecting neurons and produced a relatively modest anterograde projection to the GCD. Larger injections into the PN would undoubtedly have produced a more prominent anterograde projection. By contrast, the injection sites in the GCD involved nearly one-third of the entire volume and resulted in a relatively large number of retrogradely labeled neurons scattered throughout the PN. By inference, it seems that there is massive convergence of PN neurons into the GCD.

Role of the PN

The PN are part of one of the major pathways in the central nervous system (Brodal, 1987; for review see Schmahmann and Pandya, 1997; Schwarz and Thier, 1999). They are an important synaptic structure in the cerebral–cerebellar–cerebral circuit. The cerebral cortex sends axons to the PN, which in turn project to the cerebellum. This information is processed by the cerebellar cortex and is sent back by way of the thalamus (and other structures) to the cerebral cortex. It is worth repeating that the PN project to the cerebellar cortex in the form of mossy fibers (Ramon y Cajal, 1909; Palay, 1974), where the synaptic relationships are strikingly similar to what is observed in the GCD (Mugnaini et al., 1980a; Mugnaini, 1985; Weedman et al., 1996).

Corticopontine projections arise from almost all parts of cortex, including auditory cortex (Wiesendanger and Wiesendanger, 1982; Knowlton et al., 1993). Thus, the PN are part of the pathway that combines different kinds of cortical information to influence the output regions of the brain by way of the cerebellum (Schmahmann and Pandya, 1997). Although the cerebellum is probably the key structure in this process, the PN have been implicated in the important role of combining cortical signals with ascending afferents from subcortical sources (Leergaard et al., 2000). It has been further reported that the organization of the cortical projection to the PN is arranged in patches (Schwarz and Thier, 1999). Tracers applied to specific cortical regions label several independent areas in the PN. There is, however, some disagreement on whether the topologic spatial organization that exists in the cerebral cortex is transferred to the PN (Schwarz and Thier, 1999; Leergaard et al., 2000). One suggestion is that widely separate cortical areas can be brought together in the PN, producing the first step of a multisensory integration that is then performed by the cerebellum (Schwarz and Thier, 1999). The idea is that relevant information is

grouped together in the PN, serving to “bind” simultaneously active blocks of tissue for further processing by the cerebellum. An alternative proposal is that the cortical projections create a somatotopic map in the PN (Leergaard et al., 2000). These projections establish elongated clusters of cells that represent particular body parts, and this arrangement creates an increased interface between neighboring body representations. The result is an establishment within the PN of neighboring relationships that is not evident in the S1 body map. What remains to be determined is how brain map transformations are relayed through the PN and to what extent the PN contribute to the establishment of discontinuous (or fractured) spatial maps in the cerebellum. This question is especially pertinent to the role of these structures in the processing of acoustic information.

Role of the granule cell domain

Our study reveals a novel input to the CN granule cell domain. The PN are not classically considered part of the auditory system, although there are reports of auditory inputs to the PN (Wiesendanger and Wiesendanger, 1982; Kandler and Herbert, 1991; Knowlton et al., 1993). Neuronal responses have been recorded in the PN following acoustic stimulation in cats (Aitkin and Boyd, 1978), and it has also been shown that the PN play an essential role in conditioning animals to sound stimuli (Swain and Thompson, 1993). Thus, the PN do have auditory properties, but their function in auditory processing is unknown. The conspicuous projection to the GCD makes it very likely that they play an active role in hearing.

The granule cell domain in the CN contains a variety of different cell types, such as granule cells, Golgi cells, unipolar brush cells, mitt cells, and chestnut cells (Mugnaini et al., 1980a; Mugnaini 1985; Floris et al., 1994; Hutson and Morest, 1996; Weedman et al., 1996; Wright and Ryugo, 1996). Projections to the GCD can be divided into two major groups. One group of inputs arises from other parts of the auditory system, including type II auditory nerve fibers (Brown et al., 1988a) and projections from the superior olivary complex (Brown et al., 1988b), the inferior colliculus (Caicedo and Herbert, 1993), and the auditory cortex (Feliciano et al., 1995; Weedman and Ryugo, 1996). These inputs have been viewed as a feedback system that regulates information in the ascending auditory pathways. The other group of inputs arises from a wide range of other systems, including the trigeminal and cuneate nuclei of the somatosensory system (Itoh et al., 1987; Weinberg and Rustioni, 1987; Wright and Ryugo, 1996) and the vestibular system (Burian and Goesttner, 1988). The cells of the GCD form a complex structural circuit (Mugnaini et al., 1980b; Floris et al., 1994; Weedman et al., 1996; Wright et al., 1996; Jaarsma et al., 1998) in which the resident granule cells project exclusively to the molecular layer of the DCN (Mugnaini et al., 1980a). The granule cell axons, called *parallel fibers*, synapse on the apical dendrites of cartwheel and pyramidal cells (Mugnaini et al., 1980b; Wouterlood and Mugnaini 1984; Ryugo et al., 1995; Wright et al., 1996). Thus there is a multimodal system that modulates the output of the DCN (Davis et al., 1996). Stimulating granule cell parallel fibers in the DCN changes the response of pyramidal cells to tonal stimuli (Davis et al., 1996). Modulation of acoustic responses also occurs when the cuneate nucleus is stimulated (Saadé et al., 1989; Young et al., 1995).

Fig. 10. Electron micrographs in the granule cell domain (GCD) of the cochlear nucleus, illustrating the two types of labeled terminals. **A:** Bouton endings are small (from 1 to 2 μm in diameter) and may be differentiated from partial sections of larger mossy fibers, because they do not increase in size through serial sections. This bouton synapses (asterisk) with a dendrite of unknown origin. **B:** Mossy fiber endings are large (up to 10 μm in length), are irregular in shape, and make multiple synaptic contacts (asterisks) with dendritic profiles of unknown origin. **C:** Higher magnification view of a labeled mossy fiber (in two parts) demonstrating the asymmetry of the synaptic contacts (flanked by arrows) and the full complement of small, predominantly round synaptic vesicles. Scale bar in A = 1 μm for A,B; scale bar in C = 0.5 μm .

Thus, the output of the DCN is clearly influenced by processing in the GCD.

The question arises of the role of these various inputs to the auditory system. One idea is that input from the somatosensory proprioceptors conveys information about pinna position, head position, and body movement, and the vestibular inputs provide cues about head and body movement and position with respect to gravity. This kind of information would be important to distinguish between a stationary body around a moving sound source and a moving body around a stationary sound source. One might predict that the establishment of a dynamic auditory space map would occur early in the auditory system. The kinds of complex computations involved in such a dynamic space map would necessarily involve a variety of auditory and nonauditory systems. Interestingly, the PN is located between the cerebellum and the cerebral cortex and occupies a key synaptic position for higher order processing. Its projection to the GCD elevates the GCD as a prime candidate for the integration of multimodal signals in the ascending auditory pathway.

DCN as a cerebellar folium

Several authors have indicated the similarities between the cerebellum and the DCN (Mugnaini et al., 1980a,b; Lorente de N6, 1981; Wouterlood and Mugnaini, 1984; Mugnaini and Morgan, 1987; Berrebi et al., 1990; Ryugo et al., 1995). Not only do both structures exhibit a similar composition of cell types but also both show input by mossy fibers to granule cells. The granule cells in turn form parallel fibers that run along a molecular layer to contact the spines of apical dendrites of the resident neurons. Our study reveals another similarity between the cerebellum and the DCN in that incoming mossy fibers originate from the PN.

Do the PN provide a similar function in the pathway from cortex via the PN to the DCN as they do in the pathway from cortex to the cerebellum? The idea of an integrating function between corticopontine projections and the pontocochlear nucleus projection is supported by the anatomy of the projections. The PN receive input from almost every region of the cerebral cortex (Wiesendanger and Wiesendanger, 1982). Other authors have described input to the PN from parts of the auditory systems, including the inferior colliculus (Burne et al., 1981) and CN (Kandler and Horst, 1991). Collectively, these data suggest that various auditory nuclei and auditory cortex project to the lateral region of the PN. Terminals from other sensory areas of cortex (visual, somatosensory) are also located in the lateral region of the PN. In contrast, motor, premotor, frontal, and cingulate cortices target the medial regions of the PN. We found that the origin of the pontocochlear nucleus projection is divided into a lateral and a medial group in the PN. The lateral part of the projection might carry information from sensory parts of cortex, whereas the medial part carries signals from non-sensory parts of cortex.

Overall, the PN receive multimodal cortical information. This information is undoubtedly presented in a form that is advantageous for further processing in either the cerebellum or the DCN, but it can only be speculated what this organization might be. For example, information about head and body position necessary to create an auditory space map is thought to be integrated into the auditory system at a low level (Goossens and van Opstal,

1999). The PN circuit, however, carries information that has been highly processed by the cerebral cortex. This processing might include parts of the prefrontal and association cortex, so our idea requires a function that is under cortical control. It could involve motion detection of a sound source, which would require a constant update of expected changes in the auditory environment compared to that caused by pinna, head, or body movement. A mismatch created by an unexpected change in the sound source would alert the animal.

ACKNOWLEDGMENTS

The authors thank Tan Pongstaporn and Liana Rose for their expert technical assistance.

LITERATURE CITED

- Aitkin LM, Boyd J. 1978. Acoustic input to the lateral pontine nuclei. *Hear Res* 1:67-77.
- Berrebi AS, Morgan JI, Mugnaini E. 1990. The Purkinje cell class may extend beyond the cerebellum. *J Neurocytol* 19:643-654.
- Brodal P. 1987. Organization of the cerebropontocerebellar connections as studied with anterograde and retrograde transport of HRP-WGA in the cat. In: King JS, editor. *New Concepts in Cerebellar Neurobiology*. New York: Alan R. Liss, Inc. p 151-182.
- Brodal A, Jansen J. 1946. The ponto-cerebellar projection in the rabbit and cat: experimental investigations. *J Comp Neurol* 84:31-118.
- Brown MC, Berglund AM, Kiang NYS, Ryugo DK. 1988a. Central trajectories of type II spiral ganglion neurons. *J Comp Neurol* 278:581-590.
- Brown MC, Liberman MC, Benson TE, Ryugo DK. 1988b. Brainstem branches from olivocochlear axons in cats and rodents. *J Comp Neurol* 278:591-603.
- Burian M, Goesttner W. 1988. Projection of primary vestibular afferent fibers to the cochlear nucleus in the guinea pig. *Neurosci Lett* 84:13-17.
- Burne RA, Azizi SA, Mihailoff GA, Woodward DJ. 1981. The tectopontine projection in the rat with comments on visual pathways to the basilar pons. *J Comp Neurol* 202:287-307.
- Caicedo A, Herbert H. 1993. Topography of descending projections from the inferior colliculus to auditory brainstem nuclei in the rat. *J Comp Neurol* 328:377-392.
- Casseday HJ, Diamond IT, Harting JK. 1976. Auditory pathways to the cortex in *Tupaia glis*. *J Comp Neurol* 166:303-340.
- Davis KA, Miller RL, Young ED. 1996. Effects of somatosensory and parallel-fiber stimulation on neurons in dorsal cochlear nucleus. *J Neurophysiol* 76:3012-3024.
- Elverland HH. 1977. Descending connections between the superior olivary and cochlear nuclear complexes in the cat studied by autoradiographic and horseradish peroxidase methods. *Exp Brain Res* 27:397-412.
- Feliciano M, Saldaña E, Mugnaini E. 1995. Direct projections from the rat primary auditory neocortex to nucleus sagulum, paralemnic regions, superior olivary complex, and cochlear nuclei. *Aud Neurosci* 1:287-308.
- Fernandez C, Karapas F. 1967. The course and termination of the striae of Monakow and Held in the cat. *J Comp Neurol* 131:371-386.
- Floris A, Diño M, Jacobowitz DM, Mugnaini E. 1994. The unipolar brush cells of the rat cerebellar cortex and cochlear nucleus are calretinin-positive: a study by light and electron microscopic immunocytochemistry. *Anat Embryol* 189:495-520.
- Glendenning KK, Brunso-Bechtold JK, Thompson GC, Masterton RB. 1981. Ascending auditory afferents to the nuclei of the lateral lemniscus. *J Comp Neurol* 197:673-703.
- Goossens HH, van Opstal AJ. 1999. Influence of head position on the spatial representation of acoustic targets. *J Neurophysiol* 81:2720-2736.
- Graybiel AM. 1974. Visuo-cerebellar and cerebello-visual connections involving the ventral lateral geniculate nucleus. *Exp Brain Res* 20:303-306.
- Huffman RF, Henson OW Jr. 1990. The descending auditory pathway and acousticomotor systems: connections with the inferior colliculus. *Brain Res Rev* 15:295-323.
- Hurd LB, Hutson KA, Morest DK. 1999. Cochlear nerve projections to the

- small cell shell of the cochlear nucleus: the neuroanatomy of extremely thin sensory axons. *Synapse* 33:83–117.
- Hutson KA, Morest DK. 1996. Fine structure of the cell clusters in the cochlear nerve root: stellate, granule, and mitral cells offer insights into the synaptic organization of local circuit neurons. *J Comp Neurol* 371:397–414.
- Itoh K, Kamiya H, Mitani A, Yasui Y, Takada M, Mizuno N. 1987. Direct projections from the dorsal column nuclei and the spinal trigeminal nuclei to the cochlear nuclei in the cat. *Brain Res* 400:145–150.
- Jaarsma D, Diño MR, Ohishi H, Shigemoto R, Mugnaini E. 1998. Metabotropic glutamate receptors are associated with nonsynaptic appendages of unipolar brush cells in rat cerebellar cortex and cochlear nuclear complex. *J Neurocytol* 27:303–327.
- Kandler K, Herbert H. 1991. Auditory projections from the cochlear nucleus to pontine and mesencephalic reticular nuclei in the rat. *Brain Res* 562:230–242.
- King JS, Martin GF, Biggert TP. 1968. The basilar pontine gray of the opossum (*Didelphis virginiana*). I. Morphology. *J Comp Neurol* 133:439–445.
- Knowlton BJ, Thompson JK, Thompson RF. 1993. Projections from the auditory cortex to the pontine nuclei in the rabbit. *Behav Brain Res* 56:23–30.
- Leergaard TB, Lyngstad KA, Thompson JH, Taeymans S, Vos BP, De Schutter E, Bower JM, Bjaalie JG. 2000. Rat somatosensory cerebro-pontocerebellar pathways: spatial relationships of the somatotopic map of the primary somatosensory cortex are preserved in a three-dimensional clustered pontine map. *J Comp Neurol* 422:246–266.
- Lorente de Nó R. 1981. *The Primary Acoustic Nuclei*. New York: Raven Press.
- Manis PB. 1989. Responses to parallel fiber stimulation in the guinea pig dorsal cochlear nucleus in vitro. *J Neurophysiol* 61:149–161.
- Mihailoff GA, McArdle CB, Adams CE. 1981. The cytoarchitecture, cytology, and synaptic organization of the basilar pontine nuclei in the rat. I. Nissl and Golgi studies. *J Comp Neurol* 195:181–201.
- Mitani A, Shimokouchi M, Nomura S. 1983. Effects of stimulation of the primary auditory cortex upon colliculogeniculate neurons in the inferior colliculus of the cat. *Neurosci Lett* 42:185–189.
- Mugnaini E. 1985. GABA neurons in the superficial layers of rat dorsal cochlear nucleus: light and electron microscopic immunocytochemistry. *J Comp Neurol* 235:537–570.
- Mugnaini E, Morgan JI. 1987. The neuropeptide cerebellin is a marker for two similar neuronal circuits in rat brain. *Proc Natl Acad Sci USA* 84:8692–8696.
- Mugnaini E, Osen KK, Dahl AL, Friedrich VL Jr, Korte G. 1980a. Fine structure of granule cells and related interneurons (termed Golgi cells) in the cochlear nuclear complex of cat, rat, and mouse. *J Neurocytol* 9:537–570.
- Mugnaini E, Warr WB, Osen KK. 1980b. Distribution and light microscopic features of granule cells in the cochlear nuclei of cat, rat, and mouse. *J Comp Neurol* 191:581–606.
- Palay SL, Chan-Palay V. 1974. *Cerebellar Cortex, Cytology, and Organization*. New York: Springer-Verlag.
- Paxinos G, Watson C. 1982. *The Rat Brain in Stereotaxic Coordinates*. Sydney: Academic Press.
- Ramón y Cajal R. 1909. *Histologie du Système Nerveux de l'homme et des Vertébrés*. Madrid: Instituto Ramón y Cajal.
- Ryugo DK. 1976. *An Attempt Towards an Integration of Structure and Function in the Auditory System*. Doctoral Dissertation, University of California, Irvine, CA.
- Ryugo DK, Pongstaporn T, Wright DD, Sharp AH. 1995. Inositol 1,4,5-trisphosphate receptors: immunocytochemical localization in the dorsal cochlear nucleus. *J Comp Neurol* 358:102–118.
- Saadé NE, Frangieh AS, Atweh SF, Jabbur SJ. 1989. Dorsal column input to cochlear neurons in decerebrate-decerebellate cats. *Brain Res* 486:399–402.
- Schmahmann JD, Pandya DN. 1997. The cerebrocerebellar system. *Int Rev Neurobiol* 41:31–60.
- Schofield BR. 1990. Uptake of *Phaseolus vulgaris* leucoagglutinin (PHA-L) by axons of passage. *J Neurosci Methods* 35:47–56.
- Schofield BR, Cant NB. 1999. Descending auditory pathways: projections from the inferior colliculus contact superior olivary cells that project bilaterally to the cochlear nuclei. *J Comp Neurol* 409:210–223.
- Schwarz C, Thier P. 1999. Binding of signals relevant for action: towards a hypothesis of the functional role of the pontine nuclei. *Trends Neurosci* 22:443–451.
- Sherriff FE, Henderson Z. 1994. Cholinergic neurons in the ventral trapezoid nucleus project to the cochlear nuclei in the rat. *Neuroscience* 58:627–633.
- Shore SE, Moore JK. 1998. Sources of input to the cochlear granule cell region in the guinea pig. *Hear Res* 116:33–42.
- Shore SE, Helfert RH, Bledsoe SC Jr, Altschuler RA, Godfrey DA. 1991. Descending projections to the dorsal and ventral divisions of the cochlear nucleus in guinea pig. *Hear Res* 52:255–268.
- Spangler KM, Cant NB, Henkel CK, Farley GR, Warr WB. 1987. Descending projections from the superior olivary complex to the cochlear nucleus of the cat. *J Comp Neurol* 259:452–465.
- Swain RA, Thompson RF. 1993. In search of engrams. *Ann NY Acad Sci* 702:27–39.
- Warr WB. 1982. Parallel ascending pathways from the cochlear nucleus: Neuroanatomical evidence of functional specialization. In: Neff WD, editor. *Contributions to sensory physiology*. New York: Academic Press. p 1–38.
- Warr WB, Beck JE. 1996. Multiple projections from the ventral nucleus of the trapezoid body in the rat. *Hear Res* 93:83–101.
- Weedman DL, Ryugo DK. 1996. Projections from auditory cortex to the cochlear nucleus in rats: synapses on granule cell dendrites. *J Comp Neurol* 371:311–324.
- Weedman DL, Pongstaporn T, Ryugo DK. 1996. Ultrastructural study of the granule cell domain of the cochlear nucleus in rats: mossy fiber endings and their targets. *J Comp Neurol* 369:345–360.
- Weinberg RJ, Rustioni A. 1987. A cuneocochlear pathway in the rat. *Neuroscience* 20:209–219.
- Wiesendanger R, Wiesendanger M. 1982. The corticopontine system in the rat. II. The projection pattern. *J Comp Neurol* 208:227–38.
- Winer JA, Larue DT, Diehl JJ, Hefti BJ. 1998. Auditory cortical projections to the cat inferior colliculus. *J Comp Neurol* 400:147–174.
- Wouterlood FG, Mugnaini E. 1984. Cartwheel neurons of the dorsal cochlear nucleus: a Golgi-electron microscopic study in rat. *J Comp Neurol* 227:136–157.
- Wright DD, Ryugo DK. 1996. Mossy fiber projections from the cuneate nucleus to the cochlear nucleus in the rat. *J Comp Neurol* 365:159–172.
- Wright DD, Blackstone CD, Haganir RL, Ryugo DK. 1996. Immunocytochemical localization of the mGluR1 α metabotropic glutamate receptor in the dorsal cochlear nucleus. *J Comp Neurol* 364:729–745.
- Young ED, Nelken I, Conley RA. 1995. Somatosensory effects on neurons in dorsal cochlear nucleus. *J Neurophysiol* 73:743–765.